Polymer-Supported RNA Synthesis and Its Application To Test the Nearest-Neighbor Model for Duplex Stability†

Ryszard Kierzek,‡ Marvin H. Caruthers,*,§ Carl E. Longfellow,∥ David Swinton,⊥ Douglas H. Turner,*,∥ and Susan M. Freier∥

Institute of Bioorganic Chemistry, Polish Academy of Sciences, 60-704 Poznan, Noskowskiego 12/14, Poland, Department of Chemistry and Biochemistry, University of Colorado, Boulder, Colorado 80309, and Departments of Chemistry and Biology, University of Rochester, Rochester, New York 14627

Received June 12, 1986

ABSTRACT: A solid-phase method using a phosphoramidite approach is described for synthesis of oligoribonucleotides. The method was used to synthesize pairs of oligomers with identical nearest neighbors but different sequences. Comparison of thermodynamic parameters for these pairs provides a test of the nearest-neighbor hypothesis for prediction of helix stability. In general, pairs of sequences with identical nearest neighbors have enthalpy and entropy changes for helix formation that differ by 8% on average, ΔG°_{37} that differ by 6% on average, and melting temperatures within 0–5 °C of each other. These limits are typical of the accuracy that should be expected from nearest-neighbor predictions of RNA helix stability. UCAUGA and UGAUCA have the same nearest neighbors but melting temperatures that differ by 7 °C. This suggests some sequences will not be approximated well by the nearest-neighbor model.

The stabilities of RNA duplexes and the secondary structures of RNAs are often predicted by use of a nearest-neighbor model (Tinoco et al., 1971, 1973; Borer et al., 1974; Gralla & Crothers, 1973). Theoretical calculations support this model because they indicate base stacking is a major contributor to helix stability (Pullman & Pullman, 1968, 1969). There is little experimental evidence, however, to support the model. This is largely due to the difficulty of synthesizing suitable model oligoribonucleotides. This paper describes a rapid method for synthesizing oligoribonucleotides on a solid-phase support. The method was used to synthesize pairs of oligomers containing identical nearest neighbors but different sequences. Thermodynamic parameters of helix formation for these pairs are also reported. Comparison of these thermodynamic parameters provides a direct test of the nearest-neighbor model.

Materials and Methods

Reagents and Solvents. Silica gel H60 and Fractosil 500 were purchased from Merck. Controlled pore glass (CPG) was purchased from Pierce. Nucleosides were obtained from Pharma Waldhof.

Anhydrous solvents were obtained as follows: dichloromethane by distillation from first phosphorus pentoxide and then calcium hydride; acetonitrile by successive distillations from calcium hydride, phosphorus pentoxide, and then calcium hydride; pyridine and triethylamine by distillation from first toluenesulfonyl chloride and then calcium hydride; dichloroacetic acid (DCA)[1] and tetrahydrofuran (THF) by distillation and dimethylformamide by storage over molecular sieves followed by distillation from calcium hydride.

Thin-layer chromatography (TLC) was performed on EM plastic-backed sheets (silica gel 60 F_{254}, 0.2 mm, catalog no. 5775) in dichloromethane–methanol (9:1) (solvent A) and acetone–hexanes–triethylamine (45:45:10) (solvent B). Preparative chromatography was performed on Merck silica gel H60. Concentrations in vacuo were carried out at 40 °C or lower by using an aspirator or an oil vacuum pump. Solids were dried at 25 °C (0.02 mmHg). All reactions were at room temperature.

General Procedures. ^{31}P NMR spectra were recorded on a Bruker WM-250 spectrometer (101.2 MHz), and the chemical shifts (Hz) are reported relative to an external capillary standard of 8.5% H_3PO_4. 5′-(Dimethoxytrityl)-2′-(tetrahydropyranyl)-*N*-amide-protected nucleosides (compounds **1a–d**) were prepared according to a published procedure (Markiewicz et al., 1984). Di-*p*-methoxytrityl chloride was recrystallized from hexanes containing acetyl chloride. Tetrazole was purified by sublimation (110 °C, 12 mmHg). Diisopropylammonium tetrazolide was prepared in near-quantitative yield by dissolving tetrazole (4 mmol, 280 mg) in 10 mL of acetonitrile and adding diisopropylamine (8 mmol, 809 mg) with stirring. The product was collected by filtration, washed with dry acetonitrile, and dried in a vacuum oven (40 °C), yielding a white crystalline solid. Bis(diisopropylamino)(β-cyanoethoxy)phosphine was prepared by Dr. J.-Y. Tang from (β-cyanoethoxy)dichlorophosphine and diisopropylamine, using a published procedure (Barone et al., 1984).

Preparation of Silica Containing Covalently Attached Nucleosides (Figure 1). Compound **1a**, **1b**, **1c**, or **1d** (1 mmol), succinic anhydride (0.2 g, 1.2 mmol), and 4-(*N*,*N*-dimethylamino)pyridine (DMAP) (0.164 g, 1.3 mmol) were dissolved in 5 mL of dichloromethane and stirred for 2 h. After TLC analysis in solvent A demonstrated conversion to the corresponding succinate half-esters, each reaction mixture was diluted with dichloromethane to 7 mL. Pentachlorophenol (0.373 g, 1.4 mmol) followed by dicyclohexylcarbodiimide (0.260 g, 1.3 mmol) was then added to each reaction mixture. Analysis after 30 min in solvent A indicated complete conversion to **2a**, **2b**, **2c**, or **2d**. Reaction mixtures were quenched with 2 mL of water, stirred for 5 min and filtered to remove

† This work was supported by National Institutes of Health Grants GM22939 (D.H.T.) and GM25680 (M.H.C.).

‡ Polish Academy of Sciences.

§ University of Colorado.

∥ Department of Chemistry, University of Rochester.

⊥ Department of Biology, University of Rochester.

[1] Abbreviations: Bz_2O, benzoic anhydride; DCA, dichloroacetic acid; DMAP, 4-(*N*,*N*-dimethylamino)pyridine; DMTr, dimethoxytrityl; PAGE, polyacrylamide gel electrophoresis; THF, tetrahydrofuran.

0006-2960/86/0425-7840$01.50/0 © 1986 American Chemical Society

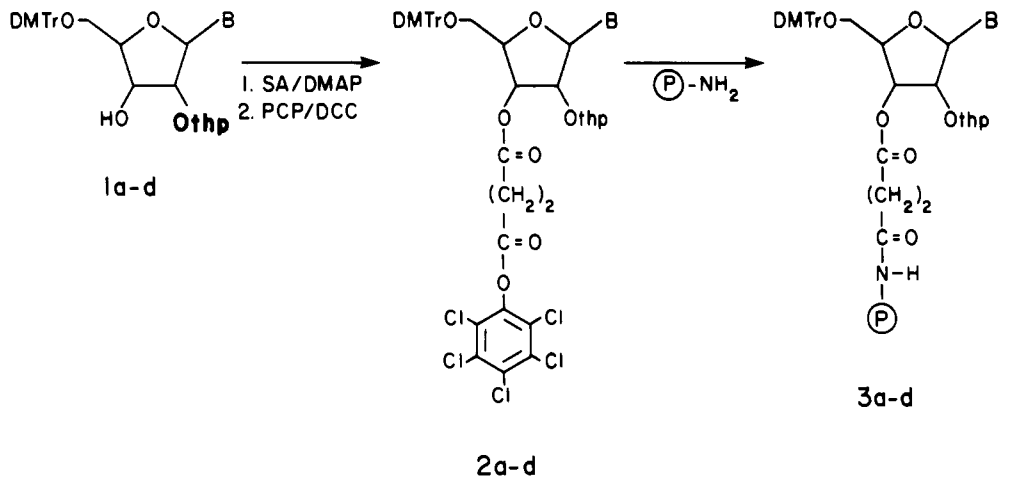

FIGURE 1: Synthesis of ribonucleosides covalently attached to silica supports: SA, succinic anhydride; DMAP, 4-(*N*,*N*-dimethylamino)pyridine; PCP, pentachlorophenol; DCC, dicyclohexylcarbodiimide; Ⓟ–NH_2, silica-based support, thp, tetrahydropyranyl; DMTr, dimethoxytrityl; B, uracil, *N*-benzoylcytosine, *N*-benzoyladenosine, and *N*-isobutyrylguanine for a, b, c, and d, respectively.

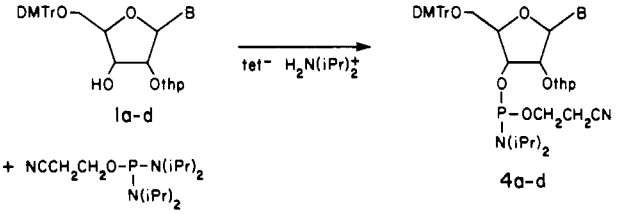

FIGURE 2: Synthesis of ribonucleoside 3′-phosphoramidites: iPr, isopropyl; tet⁻, tetrazolide.

dicyclohexylurea, diluted with 50 mL of saturated aqueous sodium bicarbonate, and extracted twice with dichloromethane (50 mL each). The combined organic layers were extracted once again with a saturated aqueous solution of NaH_2PO_4. The organic extracts from each synthesis were dried over anhydrous Na_2SO_4 and concentrated in vacuo to 2 mL. Products were recovered by chromatography on silica gel using dichloromethane–methanol (98:2 v/v) as eluant. The yield of **2a–d** was 80–85%.

Compounds **3a–d** were synthesized according to the following general procedure. Fractosil or CPG derivatized (Matteucci & Caruthers, 1980) to contain 3-aminopropylsilyl functionality (1 g; Ⓟ–NH_2 in Figure 1), **2a** (0.27 g, 0.28 mmol), and triethylamine (0.43 mL, 0.31 mmol) were added to dimethylformamide (8 mL) and shaken for 24 h. The silica support (**3a**) was collected by filtration, washed with dichloromethane and diethyl ether, and air-dried. **3a** was transferred to a round-bottom flask, and a solution of acetic anhydride–pyridine (1:9 v/v) containing DMAP (0.12 g, 1 mmol) was added. After shaking for 1 h, **3a** was isolated by filtration, washed with dichloromethane and diethyl ether, and dried in vacuo for several hours. Hydrolysis of support aliquots with acid demonstrated the silica contained 25–30 μmol of nucleoside/g (CPG) or 35–60 μmol of nucleoside/g (Fractosil). Compounds **2b–d** when reacted with silica gave comparable yields of **3b–d**, respectively.

General Procedures for Preparation of **4a–d** (*Figure 2*). Compound **1a**, **1b**, **1c**, or **1d** (1 mmol) and diisopropylammonium tetrazolide (85 mg, 0.5 mmol) were dried in vacuo for 3 h, followed by addition of acetonitrile (5 mL) and bis(diisopropylamino)(β-cyanoethoxy)phosphine (0.33 mL, 1.1 mmol). After 12 h, analysis by TLC (solvent B) indicated synthesis was complete. The reaction mixture was diluted with saturated aqueous sodium bicarbonate and extracted twice with dichloromethane (50 mL each). The combined organic extracts were washed 3 times with brine (50 mL each), dried over Na_2SO_4, and concentrated in vacuo (12 h) to a dry foam. The foam was dissolved in dichloromethane and precipitated into hexanes at −78 °C. The white precipitate was collected by filtration and dried in vacuo at room temperature. Isolated yields for **4a–d** were 90–95%. Compounds **4a–d** prepared in this manner were dissolved in anhydrous acetonitrile (0.2 M), sealed in tubes over argon, and used to synthesize RNA: ^{31}P NMR (CH_2Cl_2) for **4a**, 150.716, 150.279; for **4b**, 150.548, 149.606; for **4c**, 150.111, 149.673; for **4d**, 149.909, 149.270.

Table I: Protocol for Synthesis of RNA on Silica Supports[a]

step	reagent or solvent mixture[b]	time/step
1, 2	CH_2Cl_2 (2 mL)	30 s
3–9	DCA–CH_2Cl_2 (0.3:100 v/v) (2 mL)	1 min
10, 11	CH_2Cl_2 (2 mL)	30 s
12–16	CH_3CN (2 mL)	30 s
17	0.2 M phosphoramidite in CH_3CN (20 equiv) 0.4 M tetrazole in CH_3CN (60 equiv)	15 min
18–20	CH_3CN (2 mL)	30 s
21	THF–lutidine–H_2O (2:1:2 v/v/v) (2 mL)	1 min
22	0.1 M I_2 in THF–lutidine–H_2O (2:1:2 v/v/v) (1 mL)	30 s
23–26	CH_3CN (1 mL)	30 s
27[c]	DMAP–THF (10:90 w/v) (0.4 mL) Bz_2O–lutidine (10:90 w/v) (0.2 mL)	3 min
28–30	CH_3CN (2 mL)	30 s

[a] Syntheses were completed on Fractosil or CPG, using 1 μmol of nucleoside on the support. Reactions were carried out in a sintered-glass funnel attached to a water aspirator as the reaction vessel. Condensations were completed under an argon atmosphere. [b] The volumes are per step. [c] Bz_2O, benzoic anhydride.

Compounds **4a–d** were also prepared in situ. **1a–d** (1 mmol) and diisopropylammonium tetrazolide (85 mg, 0.5 mmol) were dried in vacuo for 3 h, followed by addition of acetonitrile (5 mL) and bis(diisopropylamino)(β-cyanoethoxy)phosphine (1 equiv). After 12 h, analysis by TLC (solvent B) indicated that each synthesis was complete. Compounds **4a–d** prepared in this manner were sealed in tubes over argon and used without isolation for the synthesis of RNA on supports.

Synthesis of RNA (*Figure 3*). RNA was synthesized manually according to the procedure outlined in Table I. Compounds **3a–d** were first converted to **5a–d**. In a typical synthesis, **3a** (20–30 mg, 1 μmol of nucleoside) was placed in a sintered-glass funnel attached to a water aspirator and washed with dichloromethane (2 × 2 mL). The support was first treated with dichloroacetic acid in dichloromethane (0.3:100 v/v, 2 mL) to convert **3a** to **5a**. Several acid steps of 1-min duration were used to facilitate monitoring the extent of detritylation. After several washes with anhydrous aceto-

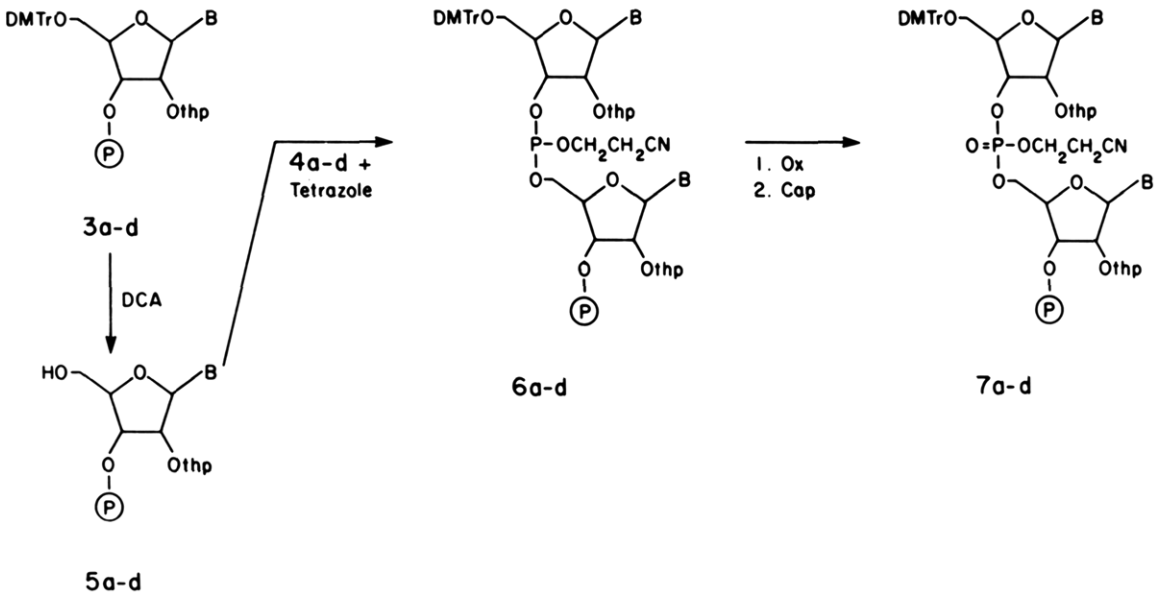

FIGURE 3: RNA synthesis procedure: Ox, oxidation; Cap, capping or benzoylation with benzoic anhydride.

nitrile, the appropriate nucleoside phosphoramidite (**4a–d**) and tetrazole were added. For example, **4a** prepared either in situ or from isolated synthons (20 equiv) as an anhydrous acetonitrile solution (0.2 M) and tetrazole (60 equiv) also as an anhydrous acetonitrile solution (0.4 M) were added to **5a**. The reaction mixture was stored over argon for 15 min, and then solvent was removed by filtration. Immediately following the condensation reaction, the product (**6a**) was washed with acetonitrile and THF–lutidine–water (2:1:2 v/v/v) and then oxidized to pentavalent phosphate (**7a**) with a solution (1 mL) of 0.1 M iodine in THF–lutidine–water (2:1:2 v/v/v). After several washes with acetonitrile (4 × 1 mL), benzoylation of unreacted 5′-hydroxyl groups was completed by adding first a solution of DMAP in dry tetrahydrofuran (1:9 w/v, 0.4 mL) and then a solution of benzoic anhydride in lutidine (1:9 w/v, 0.2 mL) to the support. After 3 min, this benzoylation solution was removed and the silica was washed with acetonitrile (2 mL). This cycle as summarized in Table I takes about 40 min and was repeated several times in order to complete the synthesis of an oligonucleotide. The yield for each condensation is about 90% based on release of the dimethoxytrityl cation.

Deprotection. Synthetic RNA was removed from the support and freed of protecting groups according to the following procedure. Concentrated aqueous ammonia (1 mL) was added to silica (20–100 mg) containing RNA and allowed to react for 2 h. After being cooled in an ice bath, the solution was transferred to a second vessel, sealed, stored at 55 °C for 20 h, and concentrated to dryness in vacuo. The dry residue was dissolved in 0.01 M HCl and the pH adjusted to 2 with 1 M HCl. After 20 h at room temperature, the reaction mixture was adjusted to pH 8 with aqueous ammonia, concentrated in vacuo to a dry residue, dissolved in 0.4 mL of water, and desalted by passage through a column of Sephadex G25. Aliquots of unpurified reaction mixtures were analyzed by phosphorylation with [γ-^{32}P]ATP and T4 kinase, followed by polyacrylamide gel electrophoresis (PAGE). Typical results are shown in Figure 4.

Purification. Oligomers were purified by ion-exchange chromatography on DEAE-Sephadex A-25. Typical gradients were 0.1–0.4 M NaCl in 7 M urea. The product is the most highly charged species in the mixture and is the last component to elute (see Figure 5). Product fractions were pooled and desalted with a Sep-Pak C-18 cartridge as described previously

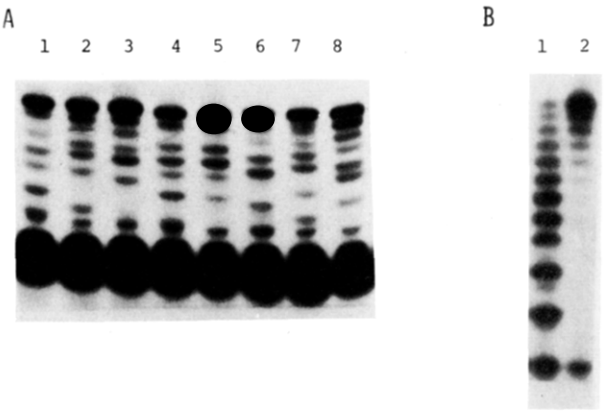

FIGURE 4: Analysis of ^{32}P-phosphorylated oligonucleotides found in reaction mixtures after complete removal of protecting groups. Both gels were 20% acrylamide and 1% *N,N*-methylenebis(acrylamide). Reaction mixtures were phosphorylated with [γ-^{32}P]ATP and fractionated by PAGE. [γ-^{32}P]ATP is the most intense band found in all lanes of panel A and has migrated off the gel in panel B. (Panel A) Lane 1, A-G-A-U-A-U-C-U; lane 2, A-U-C-U-A-G-A-U; lane 3, A-A-C-U-A-G-U-U; lane 4, A-G-U-U-A-A-C-U; lane 5, G-A-A-C-G-U-U-C; lane 6, G-U-U-C-G-A-A-C; lane 7, A-C-U-A-U-A-G-U; lane 8, A-G-U-A-U-A-C-U. (Panel B) Partially purified product from $A_{10}U_3$ synthesis after passage through Sephadex G-50. Lane 1, second part of peak. This contains primarily short fragments. Lane 2, first part of peak. This contains primarily $A_{10}U_3$.

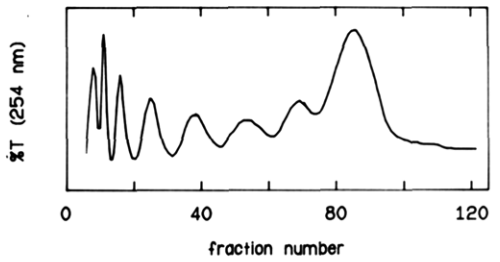

FIGURE 5: Purification of A-A-C-U-A-G-U-U. The separation of A-A-C-U-A-G-U-U from intermediates and side products was on a DEAE-Sephadex A-25 column (8 × 1.5 cm). Elution was with a 1-L gradient of 0.1–0.4 M NaCl in 7 M urea and 0.01 M Tris-HCl (pH 8.2). The fraction size was 7.5 mL.

(Freier et al., 1985). Typical yields for octamers after purification from syntheses that began with 4 μmol of nucleoside linked to silica were 0.2–0.3 μmol (15–25 OD units at 260 nm).

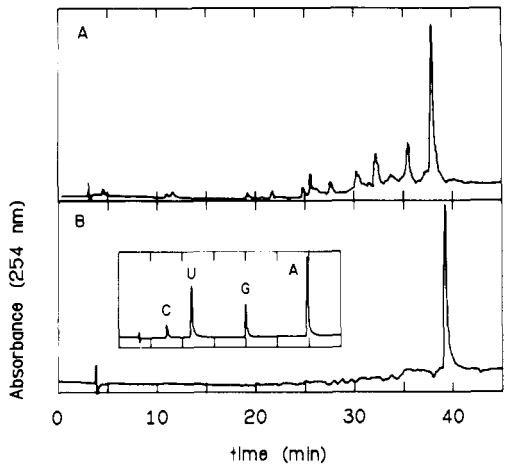

FIGURE 6: Reverse-phase HPLC profiles: (panel A) the crude product mixture in the synthesis of A-A-C-U-A-G-U-U; (panel B) elution profile of the main peak from purification on DEAE-Sephadex A-25 (Figure 5), on a 25 × 0.46 cm C-8 (Supelco LC-8-DB) reverse-phase column. The flow rate was 1 mL/min. Elution was with 0.1 M NaH_2PO_4 with a linear gradient of 0–20% methanol from 5 to 45 min. The inset shows the profile of a digest of A-A-C-U-A-G-U-U with ribonuclease T_2 and calf alkaline phosphatase.

Product Purity. Purities were confirmed by high-performance liquid chromatography (HPLC) for all oligomers (see Figure 6). For 11 oligomers, purity was confirmed by PAGE after 5′ end labeling with ^{32}P. Bands were cut out and counted. For most of these oligomers, 99% or more of the radioactivity was in the product band; for all of them, more than 94% was in the product band.

Oligonucleotides were characterized by digestion with ribonuclease T_2 and the product nucleotides 5′ end labeled with [^{32}P]phosphate. The digests were chromatographed 9 h on poly(ethylenimine) plates (Polygram Cel 300 PEI, Brinkman) in 1 M $NaHCO_2/HCO_2H$ (pH 3.5) (Randerath & Randerath, 1967). The autoradiograms showed only four spots corresponding to markers for the four major ribonucleotides, indicating the absence of modified bases.

Base compositions for GUCGAC, UCAUGA, UGAUCA, and AACUAGUU were determined by digestion to nucleosides with ribonuclease T_2 and calf alkaline phosphatase. The digests were analyzed on three different HPLC columns: (1) a C-18 reverse-phase column (Supelco LC-18-DB) eluted with 0.05 M NaH_2PO_4 and 5% methanol (pH 4.1) at 35 °C; (2) an Aminex A6 ion-exchange column eluted with 0.05 M ammonium carbonate (pH 10.0) at 50 °C (Singhal, 1972); and (3) a C-8 reverse-phase column eluted with a gradient described in Figure 6. On all three columns, only four peaks corresponding to the four major ribonucleosides were observed (see inset to Figure 6). For example, for AACUAGUU the ratio of nucleoside concentrations (A:C:G:U) from the C-8 column was 0.36:0.13:0.13:0.38, which is close to the expected ratio of 0.375:0.125:0.125:0.375. No peaks corresponding to inosine or xanthosine were observed, which demonstrates little or no deamination of adenine or guanine during synthesis.

Under the conditions of digestion, ribonuclease T_2 did not cleave a sample of adenylyl(2′–5′)adenosine. Adenylyl(2′–5′)cytidine, adenylyl(2′–5′)guanosine, and adenylyl(2′–5′)-uridine are also resistant to cleavage by this enzyme (Lapidot & Barzilay, 1972), suggesting no 2′–5′ phosphodiester bonds are cleaved by ribonuclease T_2. No peaks corresponding to dinucleoside monophosphates were observed in the chromatograms of the digests, indicating the absence of any 2′–5′ phosphodiester bonds. In addition, the profile and relative peak areas for the digestion of AACUAGUU in a solution containing snake venom phosphodiesterase, bacterial alkaline phosphatase, and DNase I were identical with that with ribonuclease T_2 and calf alkaline phosphatase. Since snake venom phosphodiesterase hydrolyzes 2′–5′ phosphodiester bonds, the identity of the two digests also demonstrates the absence of 2′–5′ linkages.

Oligonucleotide Solutions. Oligonucleotide concentrations (C_t) are strand concentrations and were calculated from the high-temperature absorbance at 280 nm. Single-strand extinction coefficients were calculated from extinction coefficients for dinucleoside monophosphates and nucleotides as described previously (Freier et al., 1983). In units of 10^4 M^{-1} cm^{-1}, calculated high-temperature extinction coefficients at 280 nm are as follows: AGAUAUCU and AUCUAGAU, 3.01; AACUAGUU, AGUUAACU, and ACUUAAGU, 3.05; GAACGUUC and GUUCGAAC, 3.57; UCUAUAGA and UAGAUCUA, 2.94; GUCGAC and GACGUC, 2.91; CAGCUGp and CUGCAGp, 2.89; ACUAUAGU and AGUAUACU, 2.96; UGAUCA and UCAUGA, 2.23. Absorbance vs. temperature profiles (melting curves) were measured in 1 M NaCl, 0.005 M Na_2HPO_4, and 0.5 mM Na_2EDTA, pH 7.

Melting Curves. The melting-curve apparatus has been described previously (Petersheim & Turner, 1983). For each oligomer, at least 16 absorbance vs. temperature melting curves were measured over a 100-fold range in strand concentration. The large concentration range is useful to precisely determine the slopes of plots of reciprocal melting temperature (T_M^{-1}) vs. log C_t. For oligonucleotides containing at least 50% G·C pairs, melting curves were measured at 280 nm; A·U-rich sequences were studied at 260 nm. For CUGCAGp, data were taken at both 260 and 280 nm. Identical thermodynamic parameters were obtained at both wavelengths.

Thermodynamic Parameters. Thermodynamic parameters of helix formation were obtained by two methods: (1) enthalpy and entropy changes from fits of individual melting curves to a two-state model with sloping base lines were averaged (Petersheim & Turner, 1983) and (2) plots of T_M^{-1} vs. log C_t yielded enthalpy and entropy changes (Borer et al., 1974).

$$T_M^{-1} = (2.3R/\Delta H^\circ) \log C_t + \Delta S^\circ/\Delta H^\circ \qquad (1)$$

We report thermodynamic parameters from plots of T_M^{-1} vs. log C_t and temperature-independent thermodynamic parameters that are the average of methods 1 and 2 (Freier et al., 1985; Petersheim & Turner, 1983).

On the basis of reproducibility, estimated error limits are ±5% for the enthalpy and entropy changes ΔH° and ΔS° and ±2% for the free energy change ΔG° at the T_M (Freier et al., 1985). Incorrect extinction coefficients could introduce an additional systematic error. A 10% error in extinction coefficient, however, results in less than 1% error in ΔG° at the T_M.

An additional source of error could arise from impure oligomer samples. To ascertain the effects of impurities on measured thermodynamics, melting curves were simulated for samples contaminated with 10% or 20% of an oligonucleotide impurity that could interact with the main species (actual impurity levels were considerably lower). In particular, melting curves were simulated for GCCGGCp contaminated with either GCCGGp or CCGGCp and for UCUAUAGA contaminated with UCUAUAG or CUAUAGA. PAGE indicated such fragments were the main contaminants. Two coupled equilibria were considered:

$$F + F \leftrightarrow F_2$$

$$F + C \leftrightarrow FC$$

Table II: Thermodynamic Parameters of Helix Formation in 1 M NaCl

	log C_T parameters				"temperature-independent" parameters			
oligomer	$-\Delta H°$[a] (kcal/mol)	$-\Delta S°$[a] (eu)	$-\Delta G°_{37}$[b] (kcal/mol)	T_M (°C) (1 × 10^{-4} M)	$-\Delta H°$[a] (kcal/mol)	$-\Delta S°$[a] (eu)	$-\Delta G°_{37}$[b] (kcal/mol)	T_M (°C) (1 × 10^{-4} M)
AGAUAUCU	64.5	187	6.58	41.4	63.4	183	6.64	41.8
AUCUAGAU	59.9	170	7.20	45.1	59.7	169	7.22	45.2
AACUAGUU	54.6	153	7.17	45.7	55.2	155	7.22	45.9
AGUUAACU	52.4	149	6.36	41.1	54.0	154	6.42	41.3
ACUUAAGU	47.2	132	6.16	40.2	49.4	139	6.24	40.6
GAACGUUC	77.0	218	9.30	52.3	74.9	212	9.21	52.4
GUUCGAAC	74.2	211	8.76	50.4	72.6	206	8.71	50.5
UCUAUAGA	62.1	178	6.96	43.6	65.3	188	6.99	43.4
UAGAUCUA	60.1	171	7.25	45.3	57.9	163	7.24	45.6
GUCGAC	53.6	150	7.09	45.4	55.4	156	7.18	45.6
GACGUC	58.1	164	7.35	46.2	57.3	161	7.34	46.3
GCCGGCp[c]	62.7	166	11.24	67.2	64.2	170	11.38	67.2
GGCGCCp[d]	67.8	182	11.33	65.2	65.6	176	11.16	65.3
CAGCUGp[e]	51.6	145	6.68	43.2	50.2	140	6.72	43.6
CUGCAGp[e]	55.4	156	7.11	45.3	54.5	153	7.11	45.4
ACUAUAGU	59.2	168	6.98	44.0	61.4	175	7.03	44.0
AGUAUACU	53.1	149	6.80	43.7	58.2	165	6.91	43.7
UGAUCA	44.7	128	5.05	32.7	45.7	131	5.09	33.1
UCAUGA	49.1	146	3.86	25.9	46.2	136	3.94	25.7

[a] Although errors in $\Delta H°$ and $\Delta S°$ are ±5%, additional significant figures are given to ensure accurate calculation of T_M. [b] The error in $\Delta G°_{37}$ can be obtained by propagation of the ±2% error in $\Delta G°$ at the T_M and the ±5% error in $\Delta H°$ to 37 °C. [c] From Freier et al. (1985). [d] From Freier et al. (1986b). [e] D. Groebe, V. Cameron, S. M. Freier, D. H. Turner, and O. C. Uhlenbeck, unpublished experiments.

where F and C represent the full-length and contaminating oligonucleotides, respectively. FC is the hybrid duplex formed from the full-length and contaminating oligomers. Duplex formation from two contaminant single strands (C_2) was ignored because of the low impurity concentrations and relatively low stability of these species. Stabilities and hyperchromicities for the hybrid duplexes were estimated from the measured effects of dangling ends (Freier et al., 1985). Melting curves were simulated for eight samples ranging 100-fold in concentration and thermodynamic parameters were obtained from these data by using the standard fitting procedures described above.

For GCCGGCp and UCUAUAGA, at impurity concentrations of 10%, $\Delta H°$ and $\Delta G°$ (37 °C) were changed less than 3% and 1%, respectively, from the values for the pure samples. When the impurity concentration was 20%, the errors in $\Delta H°$ and $\Delta G°_{37}$ were 6% and 3%, respectively, in the worst case.

There is also experimental evidence that small concentrations of oligomer impurities do not affect measured thermodynamics. Two sequences that were originally judged by gel electrophoresis to be only 77% or 88% pure, respectively, were repurified. Enthalpy and free energy changes at 37 °C measured before and after repurification changed less than 3%. It is unlikely, therefore, that oligomer impurity is increasing errors from previous estimates of ±5% in $\Delta H°$ and $\Delta S°$ and ±2% in $\Delta G°$ at the T_M.

Results

The effectiveness of the RNA synthesis method is illustrated in Figures 4–6. When compounds up to octanucleotides were synthesized, the crude reaction mixtures contained primarily product after deblocking. When longer sequences were synthesized, the reaction mixtures were dominated by failure sequences (see Figure 4B). Similar results were obtained irrespective of sequence composition. Purification on DEAE-Sephadex gave product with greater than 94% purity. Digestion of this product with ribonuclease T_2 gave only the expected ribonucleosides, indicating little or no deamination

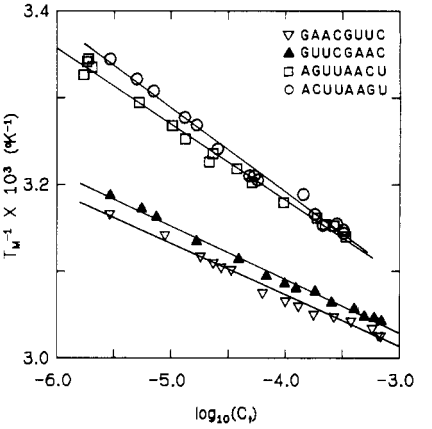

FIGURE 7: Reciprocal melting temperature vs. log (concentration) for GAACGUUC (▽), GUUCGAAC (▲), AGUUAACU (□), and ACUUAAGU (○) in 1 M NaCl, 0.005 M Na_2HPO_4, and 0.5 mM Na_2EDTA, pH 7.

or 2′–5′ phosphodiester bonds (see inset on Figure 6B).

Typical plots of T_M^{-1} vs. log C_t obtained from optical melting curves of the oligomers are shown in Figure 7. Thermodynamic parameters of helix formation obtained from these and similar plots are listed in Table II. Table II also lists temperature-independent thermodynamic parameters. The oligomers are grouped so that molecules with identical nearest neighbors appear together.

The model used to obtain thermodynamic parameters from melting data assumes the helix to coil transition is two state. Previous evidence suggests agreement between enthalpy changes from shape analysis of melting curves and those from plots of T_M^{-1} vs. log C_t is a reliable test of a two-state transition (Albergo et al., 1981; Petersheim & Turner, 1983; Hickey & Turner, 1985). Comparison of log C_t and temperature-independent parameters in Table II shows most of the oligomers studied melt in a two-state fashion; that is, enthalpies from shapes of melting curves (fitted parameters) agree within 10% with those from log C_t plots. The exceptions are AGUAUA-

Table III: Temperature-Dependent Thermodynamic Parameters of Helix Formation

oligomer	$-\Delta H^\circ_{37}$ (kcal/mol)[a,b]	$-\Delta S^\circ_{37}$[a,c] (eu)	$-\Delta C^\circ_p$ (cal mol^{-1} K^{-1})[a]
AGAUAUCU	61.0	175.5	1412
AUCUAGAU	56.8	159.3	437
AACUAGUU	53.2	147.8	740
AGUUAACU	56.9	162.7	950
ACUUAAGU	51.1	144.4	1307
GAACGUUC	68.4	190.5	308
GUUCGAAC	67.0	190.4	322
UCUAUAGA	68.7	198.2	52
UAGAUCUA	53.9	150.8	403
GUCGAC	51.8	144.4	719
GACGUC	54.2	151.3	255
GCCGGCp[d]	61.5	161.8	138
GGCGCCp[e]	58.4	154.1	185
CAGCUGp[f]	48.0	134.1	730
CUGCAGp[f]	52.2	144.1	260
ACUAUAGU	61.4	177.4	691
AGUAUACU	60.2	172.6	865
UGAUCA	47.1	135.1	512
UCAUGA	45.4	132.4	308

[a] Although estimated errors in ΔH° and ΔS° at the T_M are ±10% and errors in ΔC°_p are estimated as ±50%, additional significant figures are given to allow accurate calculation of T_M. [b] Obtained from plots of ΔH° vs. T_M. [c] Obtained from plots of ΔS° vs. ln T_M. [d] From Freier et al. (1985). [e] From Freier et al. (1986b). [f] D. Groebe, V. Cameron, S. M. Freier, D. H. Turner, and O. C. Uhlenbeck, unpublished experiments.

CU and UCAUGA, where the two methods give enthalpies that differ by 19% and 12%, respectively.

Although most of the transitions appear two state by the above criterion, a small temperature dependence is observed for ΔH° and ΔS°. Presumably, this reflects unstacking in the single-strand state (Freier et al., 1985). Values of ΔH° and ΔS° at 37 °C and of ΔC_p° were derived from plots of ΔH° vs. T_M and of ΔS° vs. ln T_M. These values are listed in Table III.

Discussion

Although the nearest-neighbor model is frequently used to predict stabilities and structures of RNA (Borer et al., 1974; Tinoco et al., 1973), it has not been tested directly. This is largely due to the difficulty in making defined-sequence oligoribonucleotides. The solid-phase method described here makes it possible to quickly synthesize short oligoribonucleotides of any sequence. The RNA is synthesized in a 3′ to 5′ direction with protected nucleoside 3′-phosphoramidites as synthons. The most important strategy decision was the choice of 2′ protecting group. Among the large number that exist, the tetrahydropyranyl group was chosen because it is free of 2′,3′ migration (Griffin et al., 1968) during synthesis of protected nucleosides and can be removed under conditions where migration of internucleotide linkages (3′–5′ to 2′–5′) occur to a negligible extent (Reese, 1985). These criteria are not met by ester protecting groups (Söll & Khorana, 1965), which gave 1–4% isomerization per internucleotide linkage in a recently reported polymer support procedure (Kempe et al., 1982). Data regarding isomerization with *tert*-butyldimethylsilyl are somewhat controversial (Jones & Reese, 1979; Kohler et al., 1978; Ogilvie & Entwistle, 1981), although it has been used to synthesize oligoribonucleotides on silica supports (Usman et al., 1985). The absence of any dinucleoside monophosphates in T_2 digests of the oligomers reported here (see Figure 6) demonstrates that essentially all internucleotide linkages remain 3′–5′ throughout the synthesis. A similar choice of tetrahydropyranyl as the 2′ protecting group has been proposed independently by Seliger et al. (1983).

Another strategy decision was choice of phosphitylating reagent. Bis(diisopropylamino)(β-cyanoethoxy)phosphine was chosen because it is stable toward oxidation and hydrolysis, unlike the corresponding chlorophosphine (Sinha et al., 1983). It is also not pyrophoric and can be activated with diisopropylammonium tetrazolide to form the nucleoside phosphoramidite without concomitant hydrolysis to the phosphinic acid or formation of the 3′–3′ isomer. In these respects, it is similar to bis(diisopropylamino)methoxyphosphine and bis(morpholino)methoxyphosphine (Barone et al., 1984).

The synthesis method readily provides quantities sufficient for optical studies. The yield per condensation is relatively low, however: ~90% based on yield of dimethoxytrityl cation, 70–80% based on isolated yield. Thus the method is probably limited to sequences shorter than dodecamers.

The thermodynamic data obtained from optical melting curves for the oligomers are listed in Tables II and III. They provide a direct test of the nearest-neighbor hypothesis since the nearest-neighbor model predicts molecules with identical nearest neighbors will have identical thermodynamic parameters for helix formation. For sequences with identical nearest neighbors, enthalpy and entropy changes from log C_t plots differ an average of 8%. This difference is about 30% larger than would be expected if it were due entirely to experimental error. For ΔG°_{37} and T_M (at 10^{-4} M), UCAUGA and UGAUCA differ by 27% and 7 K, respectively, much more than expected from experimental error. For the other pairs of sequences with identical nearest neighbors, the average differences in ΔG°_{37} and T_M (at 10^{-4} M) are 6% and 2 K, respectively, about twice that expected from experimental error. These results indicate the nearest-neighbor model is good but not perfect for the prediction of helix stability.

The pair UCAUGA and UGAUCA seems to be an exception to the generalization that molecules with identical nearest neighbors have similar stabilities. Comparison of thermodynamic parameters indicates the helix to coil transition is less two state for UCAUGA than for UGAUCA. The melting temperatures of UCAUGA and UGAUCA are respectively 9 and 2 °C less than predicted by nearest-neighbor parameters, based on results for 45 oligoribonucleotides (Freier et al., 1986a). Thus UCAUGA is less stable than expected. In studies of oligomers with internal GU mismatches, the melting temperature for CUGCGG at 10^{-4} M is 9 °C less than for CGGCUG, which has the same nearest neighbors (Sugimoto et al., 1986). This suggests a sequence YYRYGR may be unusual, where Y represents a pyrimidine and R a purine.

One model that includes more than nearest-neighbor effects is the next-nearest-neighbor model. NMR results indicate next-nearest-neighbor effects are important for determining stacking in the single strands of GUG, AUG (Lee & Tinoco, 1980), and AUAU (Altona, 1986). UCAUGA may be a sequence in which next-nearest-neighbor effects are important for determining duplex stability, perhaps because of unusual stacking in the single strand.

Another model that includes interactions beyond nearest neighbors is the R-Y model (Cruz et al., 1982; Bubienko et al., 1983). This model attributes special stability to sequences with patterns of continuous stacking. The oligomers in Tables II and III contain several pairs of oligomers with identical nearest neighbors and different stacking patterns predicted by the R-Y model. There is no correlation with stability, however.

The results in this paper indicate the nearest-neighbor model should be able to predict $\Delta H°$, $\Delta G°_{37}$, and T_M (at 10^{-4} M) for most oligomers with average deviations of roughly 8%, 6%, and 2 K, respectively. This has recently been achieved (Freier et al., 1986a). Certain sequences like UCAUGA, however, will not be well represented by a nearest-neighbor model. Further experiments are therefore required to develop a more general model for nucleic acid stability.

ACKNOWLEDGMENTS

We thank Professor Olke C. Uhlenbeck, Vicki Cameron, and Duncan Groebe for providing CAGCUGp and CUGCAGp. Prof. Uhlenbeck's unpublished experiment comparing melting temperatures of CAGCUGp and CUGCAGp provided the inspiration for comparing oligomers with identical nearest neighbors but different sequences. We thank Dr. J.-Y. Tang for many helpful discussions and for providing bis(diisopropylamino)(β-cyanoethoxy)phosphine. We also thank Dr. S. Hattman for use of his HPLC apparatus.

Registry No. **1a**, 51296-18-5; **1b**, 69359-38-2; **1c**, 71933-61-4; **1d**, 104992-60-1; **2a**, 105039-43-8; **2b**, 105039-44-9; **2c**, 105018-48-2; **2d**, 105039-45-0; **4a**, 105039-47-2; **4b**, 105018-52-8; **4c**, 105039-48-3; **4d**, 104992-58-7; **5a**, 50826-90-9; **5b**, 31505-92-7; **5c**, 31505-87-0; **5d**, 105018-53-9; AGAUAUCU, 105018-36-8; AUCUAGAU, 105018-37-9; AACUAGUU, 105018-38-0; AGUUAACU, 105018-39-1; ACUUAAGU, 105018-40-4; GAACGUUC, 105018-41-5; GUUCGAAC, 105018-42-6; UCUAUAGA, 105018-43-7; UAGAUCUA, 105018-44-8; GUCGAC, 105018-45-9; GACGUC, 103793-93-7; GCCGGCp, 97073-34-2; GGCGCCp, 101696-96-2; CAGCUGp, 103793-95-9; CUGCAGp, 103793-94-8; ACUAUAGU, 105018-46-0; AGUAUACU, 105018-47-1; UGAUCA, 105039-42-7; UCAUGA, 80969-36-4.

REFERENCES

Albergo, D. D., Marky, L. A., Breslauer, K. J., & Turner, D. H. (1981) *Biochemistry 20*, 1409–1413.

Altona, C. (1986) in *Structure and Dynamics of RNA* (van Knippenberg, P. H., & Hilbers, C. W., Eds.) Plenum, New York.

Barone, A. D., Tang, J.-Y., & Caruthers, M. H. (1984) *Nucleic Acids Res. 12*, 4051–4061.

Borer, P. N., Dengler, B., Tinoco, I., Jr., & Uhlenbeck, O. C. (1974) *J. Mol. Biol. 86*, 843–853.

Bubienko, E., Cruz, P., Thomason, J. F., & Borer, P. N. (1983) *Prog. Nucleic Acid Res. Mol. Biol. 30*, 41–90.

Cruz, P., Bubienko, E., & Borer, P. N. (1982) *Nature (London) 298*, 198–200.

Freier, S. M., Burger, B. J., Alkema, D., Neilson, T., & Turner, D. H. (1983) *Biochemistry 22*, 6198–6206.

Freier, S. M., Alkema, D., Sinclair, A., Neilson, T., & Turner, D. H. (1985) *Biochemistry 24*, 4533–4539.

Freier, S. M., Kierzek, R., Jaeger, J. A., Sugimoto, N., Caruthers, M. H., Neilson, T., & Turner, D. H. (1986a) *Proc. Natl. Acad. Sci. U.S.A.* (in press).

Freier, S. M., Sugimoto, N., Sinclair, A., Alkema, D., Neilson, T., Kierzek, R., Caruthers, M. H., & Turner, D. H. (1986b) *Biochemistry 25*, 3214–3219.

Gralla, J., & Crothers, D. M. (1973) *J. Mol. Biol. 73*, 497–511.

Griffin, B. E., Jarman, M., & Reese, C. B. (1968) *Tetrahedron 24*, 639–662.

Hickey, D. R., & Turner, D. H. (1985) *Biochemistry 24*, 2086–2094.

Jones, S. S., & Reese, C. B. (1979) *J. Chem. Soc., Perkin Trans. 1*, 2762–2765.

Kempe, T., Chow, F., Sundquist, W. I., Nardi, T. J., Paulson, B., & Peterson, S. M. (1982) *Nucleic Acids Res. 10*, 6695–6714.

Kohler, W., Schlosser, W., Charubala, G., & Pfleiderer, W. (1978) in *Chemistry and Biology of Nucleosides and Nucleotides*, pp 347–358, Academic, New York.

Lapidot, Y., & Barzilay, I. (1972) *J. Chromatogr. 71*, 275–281.

Lee, C. H., & Tinoco, I., Jr. (1980) *Biophys. Chem. 11*, 283–294.

Markiewicz, W. T., Biala, E., & Kierzek, R. (1984) *Bull. Pol. Acad. Sci., Chem. 32*, 433–451.

Matteucci, M. D., & Caruthers, M. H. (1980) *Tetrahedron Lett. 21*, 719–722.

Ogilvie, K. K., & Entwistle, D. W. (1981) *Carbohydr. Res. 89*, 203–210.

Petersheim, M., & Turner, D. H. (1983) *Biochemistry 22*, 256–263.

Pullman, A., & Pullman, B. (1968) *Adv. Quantum Chem. 4*, 267–325.

Pullman, B., & Pullman, A. (1969) *Prog. Nucleic Acid Res. Mol. Biol. 9*, 327–402.

Randerath, K., & Randerath, E. (1967) *Methods Enzymol. 12*, 323–347.

Reese, C. B. (1985) *Nucleosides Nucleotides 4*, 117–127.

Seliger, H., Zeh, D., Azuru, G., & Chattopadhyaya, J. (1983) *Chem. Scr. 22*, 95–101.

Singhal, R. P. (1972) *Arch. Biochem. Biophys. 152*, 800–810.

Sinha, N. D., Biernat, J., & Koster, H. (1983) *Tetrahedron Lett. 24*, 5843–5846.

Söll, D., & Khorana, H. G. (1965) *J. Am. Chem. Soc. 87*, 360–374.

Sugimoto, N., Kierzek, R., Freier, S. M., & Turner, D. H. (1986) *Biochemistry 25*, 5755–5759.

Tinoco, I., Jr., Uhlenbeck, O. C., & Levine, M. D. (1971) *Nature (London) 230*, 362–367.

Tinoco, I., Jr., Borer, P. N., Dengler, B., Levine, M. D., Uhlenbeck, O. C., Crothers, D. M., & Gralla, J. (1973) *Nature (London), New Biol. 246*, 40–41.

Usman, N., Pon, R. T., & Ogilvie, K. K. (1985) *Tetrahedron Lett. 26*, 4567–4570.